

## Supporting Information

### High Depolarization Temperature and Large Piezoelectricity in BiScO<sub>3</sub>-PbTiO<sub>3</sub>-Bi(Zn<sub>1/2</sub>Ti<sub>1/2</sub>)O<sub>3</sub> Piezoelectric Energy Harvesting Ceramics

Huizhong Wang<sup>a</sup>, Xiaole Yu<sup>b,\*</sup>, Mupeng Zheng<sup>a</sup>, Mankang Zhu<sup>a</sup>, and Yudong Hou<sup>a,\*</sup>

<sup>a</sup> College of Materials Science and Engineering, Key Laboratory of Advanced Functional Materials, Education Ministry of China, Beijing University of Technology, Beijing 100124, China

<sup>b</sup> College of Materials Science and Engineering, North China University of Science and Technology, Tangshan 063009, China

\*Corresponding authors.

E-mail addresses: ydhou@bjut.edu.cn (Y. Hou), xlyu66@163.com (X. Yu)

**Methods of Sample Preparation and Characterization:** Bi<sub>2</sub>O<sub>3</sub> (99%, Tianjin Fuchen chemical reagent factory), Pb<sub>3</sub>O<sub>4</sub> (99%, Tianjin Fuchen chemical reagent factory), Sc<sub>2</sub>O<sub>3</sub> (99.99%, Huizhou high purity rare earth metal materials Co, Ltd), TiO<sub>2</sub> (99%, Tianjin Fuchen chemical reagent factory), and ZnO (99%, Tianjin Fuchen chemical reagent factory) were used as raw materials. The main process flow includes ball milling, calcination (800 °C, 2 hours), granulation, pressing and sintering (1150 °C, 2 hours). X-ray diffraction (XRD; bruker D8 advance, Karlsruhe, Germany) and scanning electron microscopy (SEM; quanta 650, FEI, USA) were used to characterize the phase structure and cross section of sintered zBS-xPT-yBZT ceramics, respectively. Rietveld refinement was performed using TOfal PAttern Solution (TOPAS) software. The grain size of ceramic was measured and calculated by Nano Measurer software. The polarization process is to apply a DC electric field of 5 kV/mm to the zBS-xPT-yBZT ceramic immersed in silicone oil at 120 °C for 30 minutes. The dielectric, piezoelectric and ferroelectric properties of zBS-xPT-yBZT ceramics were characterized by commercial digital bridge (E4980A, Agilent Technologies, USA), quasi-static  $d_{33}$  tester

(ZJ-6A, China Academy of Acoustics) and ferroelectric test system (Precision Premier II, Radiant Technologies, Inc, USA). Finally, the *in-situ* high-temperature quasi-static  $d_{33}$  and high-temperature energy harvesting properties of these ceramics were measured by using the *in-situ* variable temperature  $d_{33}$  test system (TZFD-600, Harbin Julang Technology Co, Ltd) and the self-made high-temperature piezoelectric energy harvesting system.

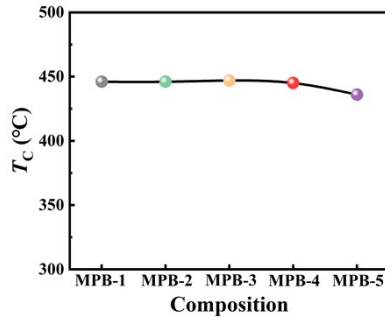


**Fig. S1** The Curie temperature ( $T_c$ ) of MPB-1~5 piezoceramics.

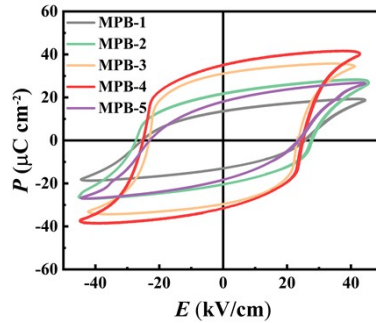


**Fig. S2** The  $P$ - $E$  loops of MPB-1~5 piezoceramics.

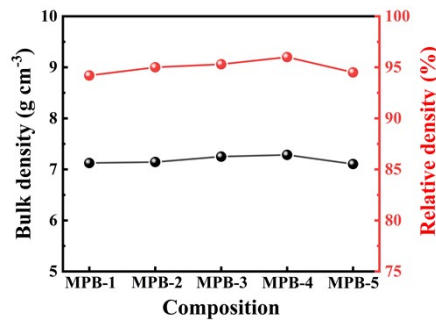


**Fig. S3** The bulk density and relative density of the  $z$ BS- $x$ PT- $y$ BZT (MPB-1~5) ceramic samples.

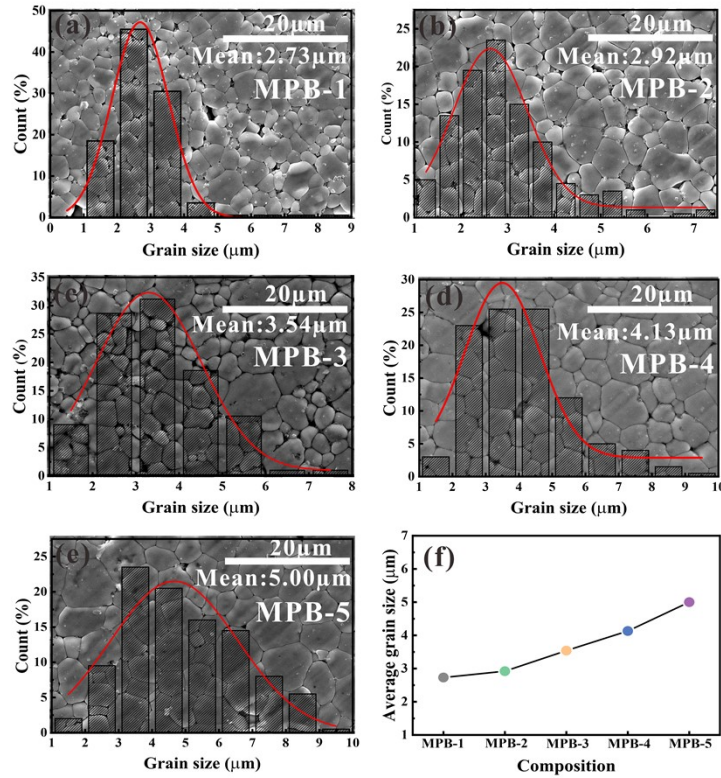


**Fig. S4** SEM images of fresh cross-section and the average grain size distributions for the zBS-xPT-yBZT ceramics: (a) MPB-1, (b) MPB-2, (c) MPB-3, (d) MPB-4, (e) MPB-5. (f) The average grain size values of the zBS-xPT-yBZT (MPB-1~5) ceramics.

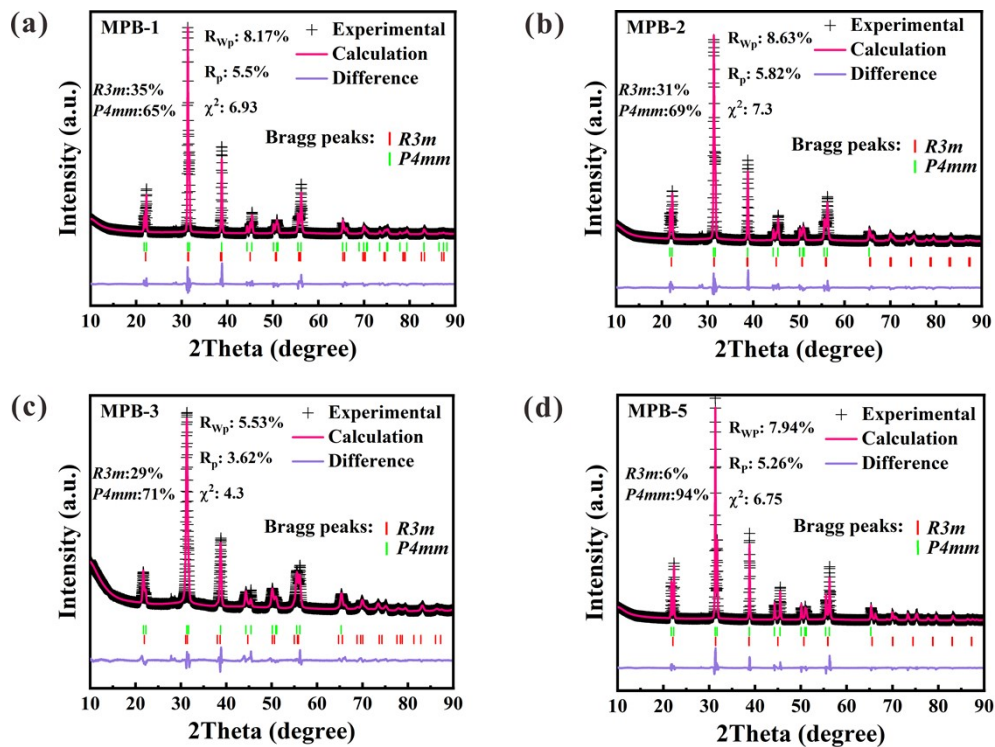


**Fig. S5** Rietveld refinement of XRD patterns for the  $z$ BS- $x$ PT- $y$ BZT ceramics: (a) MPB-1, (b) MPB-2, (c) MPB-3, (d) MPB-5

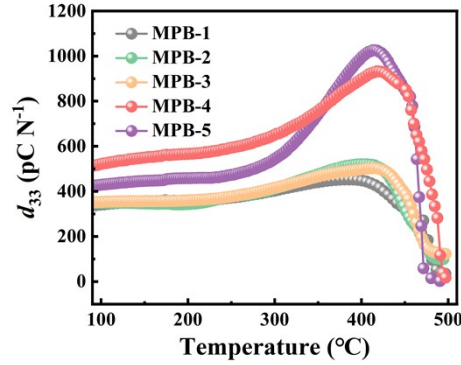


**Fig. S6** The temperature-dependent *in-situ* quasi-static piezoelectric constant  $d_{33}$  of the poled  $z$ BS- $x$ PT- $y$ BZT (MPB-1~5) ceramic samples.

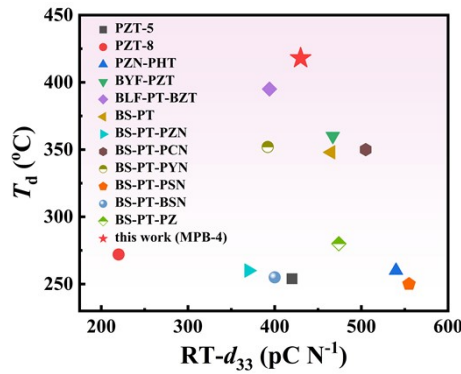


**Fig. S7** Comparison of room-temperature  $d_{33}$  and  $T_d$  between the BS-PT-BZT (MPB-4 in this work) piezoceramic and other representative lead-based perovskite piezoceramics.<sup>1-10</sup>

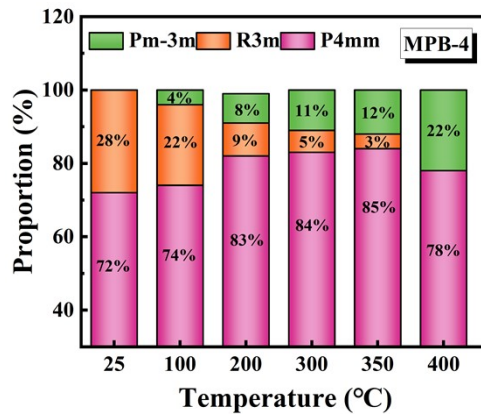


**Fig. S8** The phase proportions of the MPB-4 piezoceramic at different temperatures.

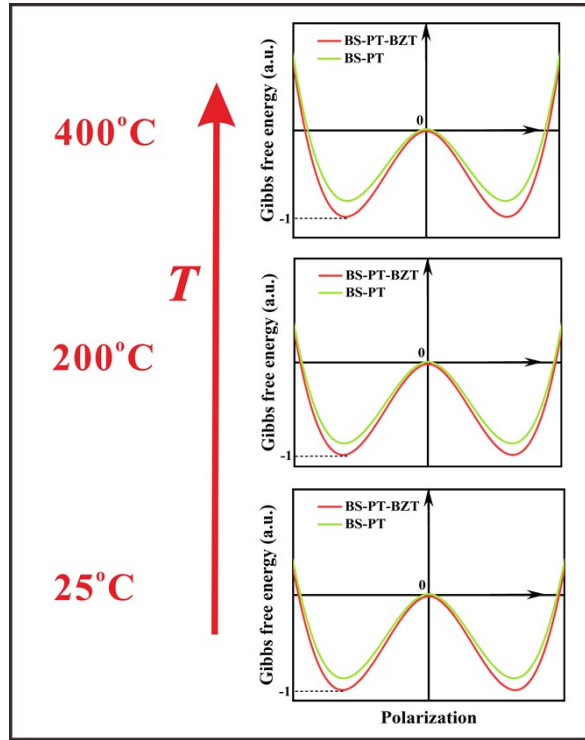


**Fig. S9** The Gibbs free energy of BS-PT-BZT (MPB-4) and BS-PT located at MPB piezoceramics.<sup>11</sup>

**Table S1.** Comparison of room temperature  $d_{33}$ , high-temperature  $d_{33}$  (measured at  $T_d$ ),  $T_d$  between the BS-PT-BZT (MPB-4, this work) piezoceramics and other typical lead-based piezoceramics<sup>1-6</sup>.

Material	$d_{33}$ (pC N <sup>-1</sup> ) at 25°C	$d_{33}$ (pC N <sup>-1</sup> ) at $T_d$	$T_d$ (°C)	Ref.
PZT-5	410	571	250	1
PZT-8	218	338	270	1
BS-PT	420	360	348	12
BS-PT-BY	438	665	348	13
BS-PT-PZ	474	430	343	7
BS-PT-BSN	450	460	275	14
BS-PT-BZH	420	762	373	11
BS-PT-BZT	430	932	418	This work

**Table S2.** The crystal structure parameters of the 0.36BS-0.62PT-0.02BZT (BS-PT-BZT, MPB-4 in this work) and the our previously reported 0.36BS-0.64PT (BS-PT64, MPB of (1-x)BS-xPT)<sup>11</sup> derived from the Rietveld refinement at different temperatures.

Materials	$T_{\text{test}}$ (°C)	Space group	Phase content (%)	$a$ (Å)	$c$ (Å)	$R_{\text{wp}}$ (%)	$R_{\text{p}}$ (%)	$\chi^2$
BS- PT64 <sup>11</sup>	200	<i>P4mm</i>	72	4.0037	4.0745	6.32	4.58	3.26
		<i>R3m</i>	28	4.0380	4.0380			
	400	<i>P4mm</i>	60.5	4.0191	4.0631	7.15	5.04	
		<i>R3m</i>	39.5	4.0312	4.0312			
BS-PT- BZT	200	<i>P4mm</i>	83	4.0010	4.0771	8.82	6.09	6.78
		<i>R3m</i>	9	4.1219	4.1219			
	400	<i>Pm-3m</i>	8	4.0149	4.0149	9.53	7.2	
		<i>P4mm</i>	78	4.0170	4.0651			
		<i>R3m</i>	0	0	0			
	<i>Pm-3m</i>	22	4.0245	4.0245				

**Table S3.** Related parameters for Gibbs free energy calculations.<sup>5, 15</sup>

$\alpha_{ijk}$ coefficient	Formulas and values
$\alpha_1$	$\alpha_1(T) = \frac{T - T_0}{2\varepsilon_0 C}$
$\alpha_{11}$	$3.614 \times 10^7 \text{m}^5/\text{C}^2\text{F}$
$\alpha_{12}$	$3.233 \times 10^8 \text{m}^5/\text{C}^2\text{F}$
$\alpha_{111}$	$1.859 \times 10^8 \text{m}^9/\text{C}^4\text{F}$
$\alpha_{112}$	$5 \times 10^8 \text{m}^9/\text{C}^4\text{F}$
$\alpha_{123}$	$-3.5 \times 10^9 \text{m}^9/\text{C}^4\text{F}$

## Reference

1. F. Li, Z. Xu, X. Wei and X. Yao, *J. Electroceram*, 2009, **24**, 294-299.
2. Q. Liao, X. Chen, X. Chu, F. Zeng and D. Guo, *Sens. Actuator A-Phys*, 2013, **201**, 222-229.
3. Z. Lan, J. Liu, S. Ren, X. Jiang, K. Chen, L. Fang, B. Peng, D. Wang and L. Liu, *J. Mater. Sci*, 2019, **54**, 13467-13478.
4. H. Zhao, Y. Hou, X. Yu, J. Fu, M. Zheng and M. Zhu, *J. Am. Ceram. Soc*, 2019, **102**, 5316-5327.
5. T. L. Zhao, A. A. Bokov, J. Wu, H. Wang, C. M. Wang, Y. Yu, C. L. Wang, K. Zeng, Z. G. Ye and S. Dong, *Adv. Funct. Mater*, 2019, **29**, 1807920.
6. Y. Dong, Z. Zhou, R. Liang and X. Dong, *J. Am. Ceram. Soc*, 2021, **105**, 1558-1567.
7. H. Yin, Y. Wang, B. Kuang, B. Yuan, L. Mao, H. Ma, Q. Hu and J. Huang, *J. Mater. Sci.-Mater. Electron*, 2021, **32**, 6047-6054.
8. X. Yu, Y. Hou, M. Zheng and M. Zhu, *J. Mater. Chem. A*, 2021, **9**, 26741-26749.
9. M. Gao, Z. Yu, J. Fu, Y. Zhang and R. Zuo, *J. Mater. Sci.-Mater. Electron*, 2023, **34**, 1085.
10. Y. Huang, L. Zhang, R. Jing, M. Tang, D. Alikin, V. Shur, X. Wei and L. Jin, *Chem. Eng. J*, 2023, **477**, 147192.
11. H. Zhao, Y. Hou, X. Yu, M. Zheng and M. Zhu, *J. Mater. Chem. A*, 2021, **9**, 2284-2291.
12. C. Huang, K. Cai, Y. Wang, Y. Bai and D. Guo, *J. Mater. Chem. C*, 2018, **6**, 1433-1444.
13. H. Zhao, X. Yu, Q. Guo, H. Yang, F. Li, S. Zhang and X. Wu, *J. Mater. Chem. C*, 2023, **11**, 16536-16544.
14. Y. Dong, Z. Zhou, R. Liang and X. Dong, *J. Materiomics*, 2022, **8**, 319-326.
15. M. J. Haun, Z. Q. Zhuang, E. Furman, S. J. Jang and L. E. Cross, *Ferroelectrics*, 1989, **99**, 45-54.